Investigation of a solar cooling and process heat system in hot climates for steam, heat and cold supply in industry

Uli Jakob[1] and Michael Strobel[1]

[1] Dr. Jakob energy research GmbH & Co. KG, Weinstadt (Germany)

Abstract

This paper analyses a solar cooling system including a hybrid heat pump (HHP) and concentrating Fresnel collector plant of 400 m^2 for industrial purpose at four different locations in hot climates (Barcelona in Spain, Johannesburg in South Africa, Mexico-City in Mexico and Cairo in Egypt). The HHP consists of adsorption chillers (AdC) and compressions chillers (CC) connected in series. This design combines the benefits of both technologies, as the solar thermally driven AdCs work in most efficient temperature levels and the CCs only provides the remaining cooling load. The TRNSYS simulation concluded that the operation in Johannesburg shows best performance in total numbers, accounting more than 160 MWh/a solar yield, as well as the steadiest provision of cold throughout the year. The AdCs in the system cause a significant increase of the electrical Energy Efficiency Ratio (EER_{el}) of the CCs by up to 20 %. Furthermore, a connected steam network at the industrial sites serves as heat storage to provide stored solar heat even at night-time. That means that the solar thermally driven chillers have the potential to operate even in night times, resulting in most efficient operation thanks to lower ambient air temperatures. The COP_{th} of the AdC is between 0.45 and 0.50 for Johannesburg and Mexico-City. The increased efficiency of the CCs and solar generated cooling capacity cause a reduction in electricity consumption. This again leads to potential savings of CO_2 emissions. The calculated savings for Johannesburg account more than 50 t/a. The conclusion of the paper is, that the investigated solar cooling system shows best energetic and technical performance for applications in South Africa.

Keywords: Solar cooling, solar process heat, solar steam generation, hybrid heat pump, adsorption chiller, heat rejection, energy analysis, TRNSYS, steam network simulation

1. Introduction

Energy saving and energy efficiency actions are crucial to lower the world's greenhouse gas (GHG) emissions. More than 20 % of direct GHG emissions can be traced back onto the industrial sector. By attributing further emissions from electricity and heat production this share increases to 31 % GHG emissions in total (Pachauri and Meyer, 2014). Renewable energy, in fact solar energy, shows a potential of 5.6 EJ/a in 2050 (UNIDO, 2010) in industrial process heat. Here, the food sector has the major share with 46 %. Currently, the share of Renewable Energies (RE) in the food sector accounts only about 4 %, which is used almost completely in process heat (Eurostat, 2018). However, electricity is second most consumed energy source in food industry with 34 %. Generation of cold here is again the most required form of usage accounting 31 %, see Figure 1. In total, supply of cold accounts 11 % of energy consumption in the food industry (Monforti-Ferrario et. al, 2015). This share differs significantly from one product to another. At this point, the use of solar cooling promises savings in both GHG emissions and primary energy consumption. Concentrating solar systems generating steam are capable to function as a heat source for both process heat and process cooling and show great possibilities of application in the food industry. This paper analyses such a system, in particular with regard to its cooling performance and its possible use in a global context.

10.18086/swc.2023.04.08 Available at http://proceedings.ises.org

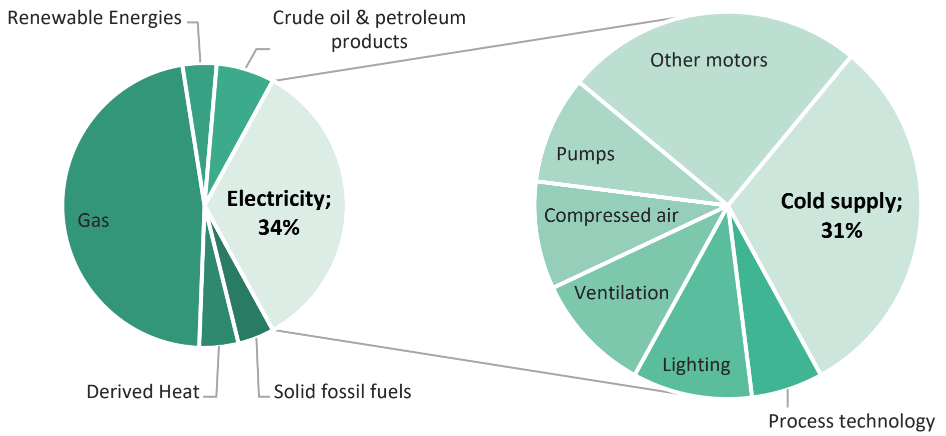

Figure 1: Distribution of total energy consumption and electricity consumption in the food industry. Adapted from (Eurostat, 2018) and (Monforti-Ferrario et. al, 2015) (Source: JER)

2. Weather data analysis

The analysis explores four different locations on three different continents: Europe, Africa and North America. The locations are the cities of Barcelona (Spain), Cairo (Egypt), Johannesburg (South Africa) and Mexico-City (Mexico). A preliminary analysis of the weather conditions for each city is conducted. Each location represents dry weather with hot summers and mild winters, as the temperature ranges show in Figure 2. In addition to the hot temperatures, the chosen global locations have good conditions in terms of Global Horizontal Irradiation (GHI).

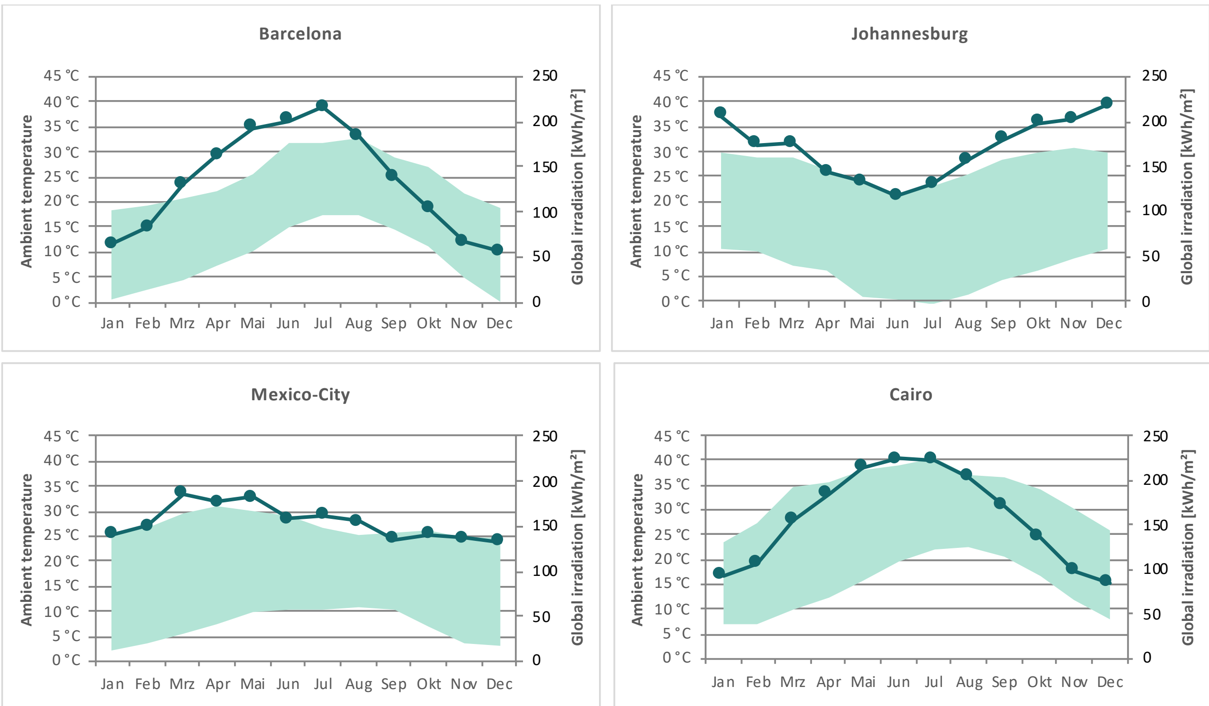

Figure 2: Investigated weather data (ambient air temperature range and global irradiance) for the four global locations.

Mexico-City is the location closest to the equator, followed by Johannesburg, then Cairo and the city farthest away from the equator is Barcelona. The relationship of the locations in context to the distance to the equator can also be seen in the range of the GHI over the year, as the range of the GHI in Barcelona is the most diverse and the GHI in Mexico-City is the steadiest over the year. The yearly sum of GHI is in Johannesburg the highest with 2,036 kWh/m²a and the lowest in Barcelona with 1,600 kWh/m²a. Cairo and Mexico-City show here a similar sum of 1,898 kWh/m²a and 1,859 kWh/m²a, respectively.

Taking into account the temperature levels, Cairo shows the hottest temperature with a maximum of 40 °C, which is up to 10 K higher than in Mexico-City and Johannesburg or about 8 K higher than in Barcelona. Furthermore, as Johannesburg is the only location of the four investigated ones, located on the Southern hemisphere, so it is the only one with higher GHI and higher temperatures from September to March, whereas especially Cairo and Barcelona show high temperature ranges and GHI from April to September. Table 1 also shows the annual direct normal irradiation (DNI) per location.

Table 1: Comparison of annual DNI for the four global locations.

Barcelona	**Johannesburg**	**Mexico-City**	**Cairo**
1,737 kWh/m^{2}a	2,130 kWh/m^{2}a	2,055 kWh/m^{2}a	2,039 kWh/m^{2}a

3. Investigated solar cooling system

3.1 Design approach

The investigated solar cooling system follows basically the design of the HyCool project using innovative hybrid chillers (Frazzica et. al, 2020). The system will provide both heat and cold for industrial purposes. Several unique features, such as concentrating solar collectors, steam generation, latent heat storage, adsorption chiller, compression chiller, as well as steam, hot water and chilled water circuits are combined within the system, what makes the system so innovative. The schematic design of the system, using two Fresnel collector fields and providing finally both heat and cold, is shown in Figure 3.

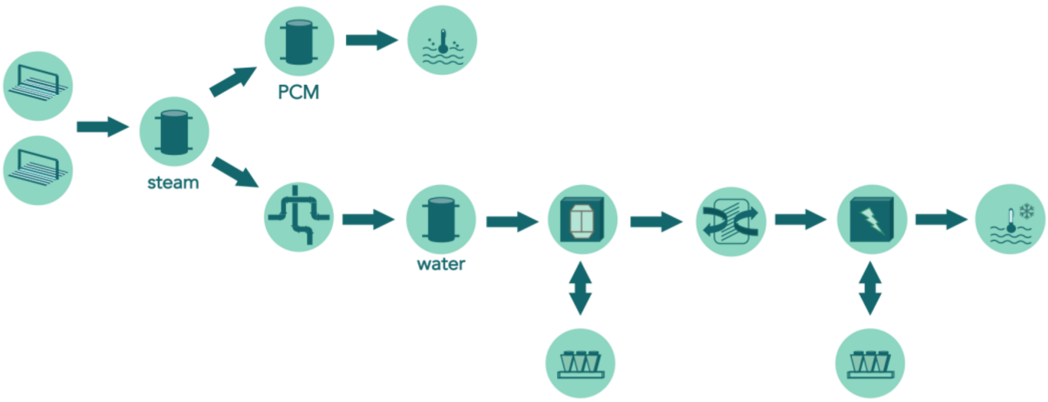

Figure 3: Schematic design of the solar cooling system. (Source: JER)

It contains two fields of concentrating Fresnel collectors providing steam at 25 bar. The steam then will be forwarded to a steam drum, with a 0.5 m^3 volume, separating liquid elements from the gaseous steam. The first solar generated steam of the day is forwarded to a latent heat storage using phase change material (PCM) for industrial heat usage at night-time. Once the storage is fully charged, the system switches to supply the local already existing industrial steam network. The steam network, operating at a pressure level of 20 bar, which supplies heat to a hot water storage. This storage serves as heat source for the thermally driven chillers. The so called HHP storage tank has a volume of 5 m^3. The core of the system is the energy efficient combination of adsorption chillers and compression chillers. Designed in a series connection, the adsorption chillers pre-cool the return flow of the chilled water-glycol mixture, in order that the conventional compression chillers must provide less cooling capacity and thus save electricity accompanied by GHG emissions. However, the chilling cycle is divided into two cycles. The compression chillers is placed directly in the chilling cycle circulating the water-glycol mixture, whereas the adsorption chillers serve a chilled-water cycle which is connected via a heat exchanger to the glycol-water mixture cycle.

Two adsorption chillers are designed with a cooling capacity $\dot{Q}$chill of 32 kW each under nominal conditions. These chillers are operated with heat from the HHP storage tank with hot water of 85 to 90 °C. The adsorption chillers work in a discontinuous process, resulting in a non-steady chilled water temperature level. The design of the system takes into account, that adsorption chillers show best performance and efficiency when they work with chilled water temperatures at a moderate level. Thus, the AdCs cool the chilled water in a first step from 12 °C down to 8 to 12 °C. The cooling capacity of the AdCs is affected by the provided heat level, the heat rejection and chilled water temperature. In a second step, then the CCs cool down the chilled water to 5 °C to reach in a steady way the targeted process temperature.

Another design approach for the solar cooling system with an HPP, using a cascade configuration of the AdC and CC, was investigated in detail for industrial applications below 0° C in Spain and showed an EER_{el} of 7-8 at ambient air temperature of 36-37°C (Jakob, et. al, 2018).

3.2 Modelling and simulation of the system

The system described was modelled with the simulation program TRNSYS 17. The subject of the simulation is to display the energetic performance throughout the year and to calculate the annual cooling yield. Therefore, emphasis was put on including all components affecting the thermal and energetic performance of the system, such as pressure conditions, specific storage and beyond. Since the focus is on the analysis of possible location and weather-related differences, the mass flows and further processing of steam, hot and chilled water is of great importance.

Table 2: Overview of used TRNSYS types referring to their role in the system simulation.

Component	Type
Concentrating solar collector	Type 1288
Evaporator	Type 1998
Adsorption chiller	Type 820
Compression chiller	Type 666
Evaporation water tank	Type 534
Storage representing PCM storage	Type 60c
HHP storage	Type 60t
Virtual storage (steam network)	Type 60c
Heat exchanger	Type 91
Glycol tank	Type 4e
Pumps	Type 3b

Within the simulation model, the concentrating Fresnel collectors are modelled using Type 1288 in order to calculate the transferred solar energy for heating the heat transfer fluid with its properties. Since Type 1288 doesn't have the potential to work with a fluid in two phases, including its evaporation from liquid to gaseous, the evaporation of the fluid must be modelled separately. Type 1998 is used for this purpose, which is a steam evaporator that calculates the evaporation rate including the resulting mass flows on steam side as outlet and feed water in relation to the entered pressure level and the associated enthalpy of evaporation. The collector model therefore doesn't consider the evaporation temperature, but supplies heat to the collector fluid, which in a further step evaporates the fluid, in this case water, in relation to the supplied heat. At the pressure level of 25 bar, the evaporation enthalpy is 1,860 kJ/kg. According to this calculation method, superheating of the steam is not taken into account. Since the pressure level and thus the resulting evaporation temperature are fixed, the mass flow varies depending on the solar irradiation and the solar collector output. However, before the thermal energy is fed to the evaporator, the evaporation water tank with a volume of 0.5 m^3 is heated up with the collector fluid. Thus, the combination of tank and evaporator simulates the steam drum.

From there on, only the steam mass flow is considered. The first 200 kWh of steam are supplied to the storage tank by the steam evaporator type 1998. At night, the storage tank is discharged from 1 a.m. so that the stored heat can also be used at night. The design of the storage tank and the further use of the heat is not part of the detailed investigation of the performance of the solar cooling system. However, the piping to the storage tank is taken into account as steam condenses within the piping due to heat losses from the piping. This condensate is fed to the Type 1998 as feed water.

Once the storage tank is charged, the rest of the solar generated steam is fed into the existing steam network of the industrial plant. This steam network is actually considered as a virtual storage. This storage carries the solar generated steam and provides heat to the HHP storage tank until it reaches a maximum temperature of 96 °C to avoid boiling. In fact, the virtual storage tank transfers as much heat to the HHP storage tank as solar heat was generated. The loading capacity is therefore limited to the accumulated solar heat that is available.

Type 820 is used for the water/silica gel adsorption chillers. Thanks to the HHP storage tank, heat is supplied to the AdC at a constant temperature between 90 and 95 °C. Under nominal conditions, the AdC has an output of 32 kW cooling capacity. The design of the CCs is based on the data of the Multichiller MCL 78-3 E with a cooling capacity of 50 kW and an EER_{el} of 3.21. For reasons of simplification, the type of heat rejection is constant for each simulated location. The heat rejection inlet temperature of the chillers is set to 5 K above the ambient air temperature. The adsorption chiller Type 820 simulates the operation of a two-chamber adsorption chiller, including internal evaporator and condenser. Thus, both the process of desorption and adsorption are considered. In fact, this requires a simulation in equivalent time steps. In detail, the duration of each cycle, the time of the thermal regeneration of the sorption material and the duration of the exchange of the cycle process must be specified. Since the duration for the exchange is the shortest (10 seconds), this defines the minimum time step of the entire simulation. This short time step combined with the duration of the investigated system simulation results in a data set of 3,153,600 per unit.

Table 3: Characteristics of used heat transfer fluids.

Heat transfer fluid	Density	Spec. heat capacity	Application
Water	1,000 kg/m^3	4.19 kJ/kgK	heat supply AdC, chilling cycle AdC
Glycol 34	1,045 kg/m^3	3.67 kJ/kgK	heat rejection cycle AdC, heat rejection cycle CC
Glycol 50	1,085 kg/m^3	3.27 kJ/kgK	chilling cycle, CC

The entire chilling process focuses on cooling down the heat transfer fluid, a water glycol mixture with 50 % glycol, in the chilling cycle to a target temperature of 5 °C. The heat rejection cycles of both AdC and CC runs with Glycol 34. Both the density and the specific heat capacity are adapted following the specifications in Table 3. The chilled fluid is stored in the glycol tank with a storage volume of 5 m^3. Since the simulation aims to use the generated solar energy whenever and for as long as possible, the mass flow of the chilling cycle runs continuously. This means, that the CCs also run permanently. Since the investigation of the system performance only focuses on the solar performance, the permanent operation of the chilling cycles doesn't affect the entire investigation. However, the return flow temperature of the chilled fluid is fixed at 14 °C. In connection with the assumed mass flow of 20,000 kg/h glycol mixture, the permanent cooling capacity demand is 127.2 kW. This definition was based on the fact, that the four CCs, each with a cooling capacity of 50 kW, are able to provide the desired cooling capacity without the support of the solar thermally driven AdCs. In addition, since the cooling demand can vary greatly, no detailed study of the use of the chilled fluid has been made. In fact, this limit improves the scalability and comparability of the individual simulation results.

Figure 4 shows the entire simulation deck in TRNSYS 17. The simulation can be understood from the upper left corner to the lower right corner. To make the system easier to understand, cold fluid flows in a cycle are shown in blue and hot flows in red. Heat rejection cycles are shown in green.

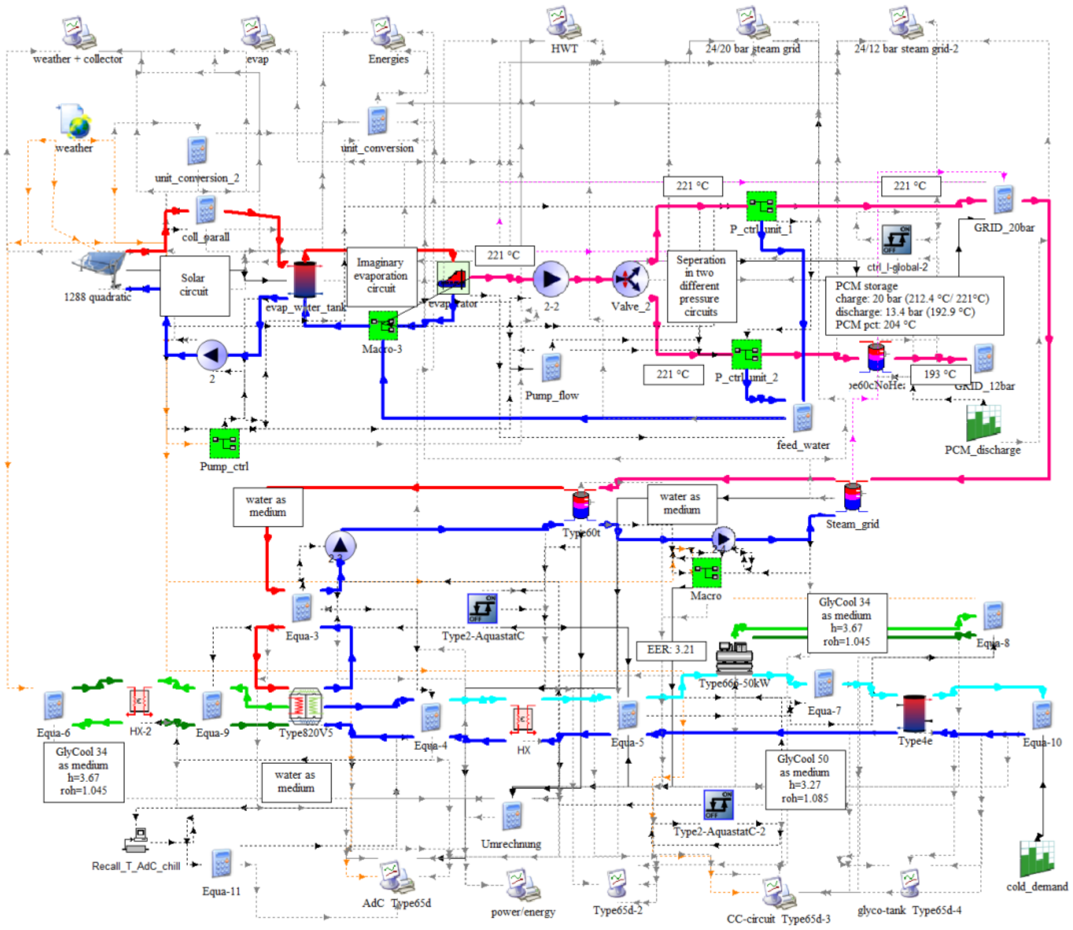

Figure 4: TRNSYS deck of the solar cooling HHP system. (Source: JER)

A detailed analysis of the hydraulics and the pressure conditions in the system as well as the design of the heat exchanger was not carried out. It is expected that these aspects will not results in differences in the performance of the HPP system at different locations. In addition, the power consumption for the various components in the system is also not part of the performance study.

4. Results

First, the weather data conditions were analyzed, secondly the results of the four TRNSYS simulations and finally an assessment of relevant Key Performance Indicators (KPIs) for each location. The results of the simulations are evaluated with regards to EER_{el} and Global Warming Potential (GWP).

According to the weather data, Johannesburg shows the best boundary conditions for the performance of the solar cooling system. The temperature profile reaches the lowest temperatures of all the locations examined. Both sets of weather data for Mexico-City and Cairo have a similar GHI, a similar irradiation, but Cairo shows the highest ambient air temperature of all locations, which anticipates a reduction in the cooling capacity of the chillers. Barcelona has the greatest variance in solar irradiation over the course of the year and also the lowest GHI of the four investigated locations, which means that the lowest solar yield with the lowest cooling yield can be expected.

4.1 Daily analysis

The analysis of the course of a day basically shows the influences and process of solar thermal energy in the simulation. The trends in the Figure 5 show a 48-hour period for December 21 and 22 for the Johannesburg location, including the summer solstice. It shows the performance curves of the solar collector system, the PCM storage loading and the cooling capacity of both AdCs. First, the solar collector system generates heat, which is further distributed to the evaporator in the TRNSYS simulation deck to generate steam. The evaporation water tank (steam drum) is then preheated and the loading of the PCM storage begins. The loading process then takes a little over an hour. The loading curve runs below the solar collector curve, since the PCM storage trend only represents the steam capacity produced. As soon as the PCM storage is fully loaded with 200 kWh, the loading process stops. The capacity of the solar collectors increases during the day and drops briefly at noon. This drop is caused by the design of the concentrating Fresnel collector field, which is oriented in a north-south direction. In fact, in good weather conditions, the solar concentrating collectors provide heat for the system for eleven hours.

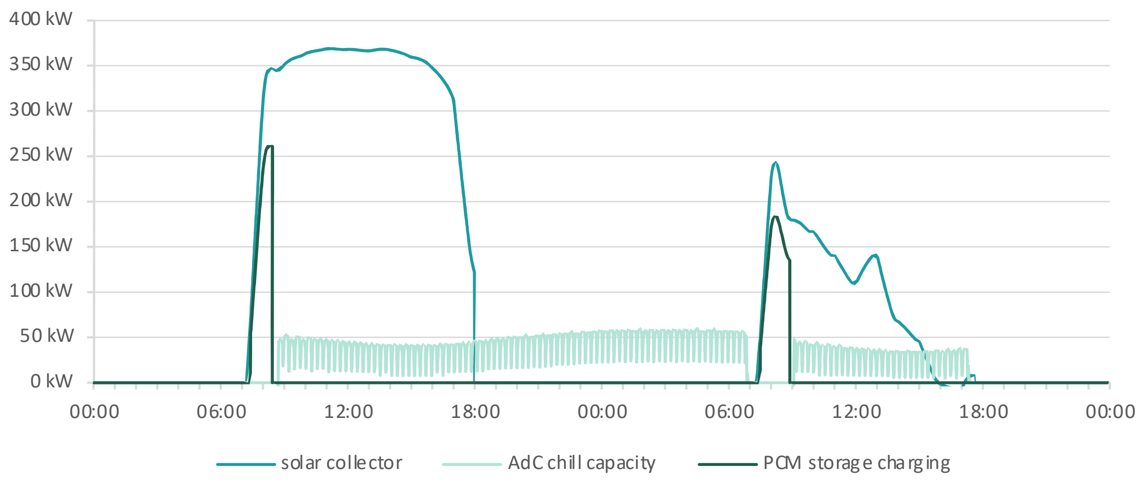

Figure 5: System performance trend for 48 hours.

The operation of the AdCs starts as soon as the PCM storage is fully loaded. The two AdCs then run until shortly before the next solar heat generation the next morning. This shows the effects of storing the solar generated steam in the steam network of the industrial site, which makes it possible to run the chillers at night as well. Moreover, the chillers run more efficiently at night, which can be seen in the higher cooling capacity output. At night, the ambient air temperature is lower than during the day, which affects the heat rejection temperature of the dry cooler. As already explained, the heat supply of the AdC is designed for a constant supply of heat. The next day, the conditions for the solar yield of the collectors are not optimal, since the solar irradiation is not as high during the day and it decreases further during the day. But it can be clearly seen that the PCM storage is fully charged by 10 a.m. After that, the solar thermal output is only used to operate the adsorption chillers. Since the solar irradiation doesn't provide heat as on the first day, the AdCs stop operating before 6 p.m.

4.2 Monthly and annual analysis

Figure 6 shows the monthly sum of the solar collector yield, the heat supplied to the AdCs and finally the sum of the cooling capacity generated by the AdCs. The performance of the systems correlates well with the weather analysis, in fact with the trends of the solar irradiation. The monthly solar yield of the concentrating collector field reaches a maximum of 50 MWh or even more in each investigated location. The overall maximum of the solar yield across all location is found in January in Johannesburg with 53.9 MWh.

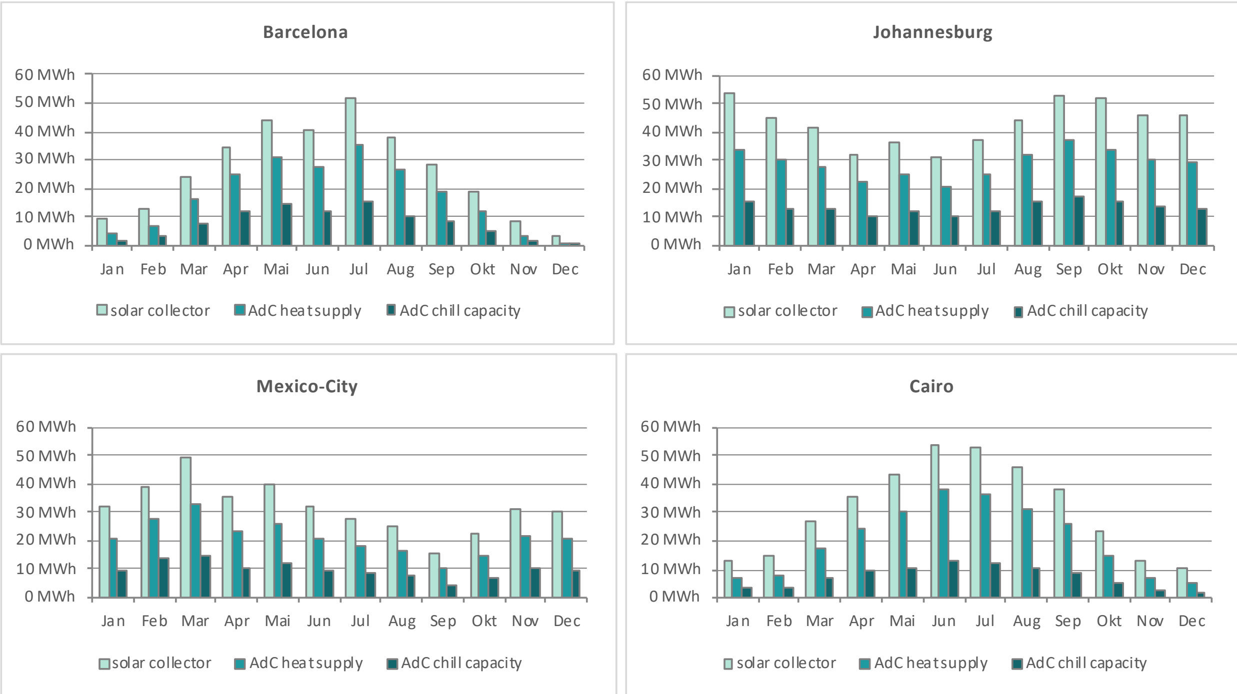

Figure 6: Monthly system performance results for Barcelona, Johannesburg, Mexico-City and Cairo.

According to the system design, the yield shown above includes preheating of the water to the evaporation temperature and subsequent boiling. The heat supplied shown in the four graphs is similar to the steam distributed to the "virtual steam network". The last bar provides information about the actual cooling performance of the AdCs. All year round, Johannesburg has the very best performance as it is the only location where the cooling capacity never drops below 10 MWh per month. In terms of yield, Johannesburg is the best location, followed by Mexico City. Cairo hardly shows a greater yield than Barcelona, where solar cooling has little to no effect in the winter months (0.1 MWh).

Comparing the total amount of cold generated over the year in Figure 7, Johannesburg has by far the best performance with 162.0 MWh. Compared to Mexico City, an additional 45 MWh of cold can be generated for the Johannesburg location in South Africa. The performance of the systems for the Barcelona and Cairo locations shows a similar annual cooling capacity: 90.2 MWh in Barcelona and 87.4 MWh in Cairo. Although Cairo has more solar irradiation and higher solar yield compared to Barcelona, the chilling process is less productive and less efficient. The weather in Cairo is the hottest of all weather data sets examined. As the heat rejection process of the chillers depends largely on the ambient air temperature, the heat rejection temperature is higher than at other locations. This leads to a reduction in the COP of the chillers.

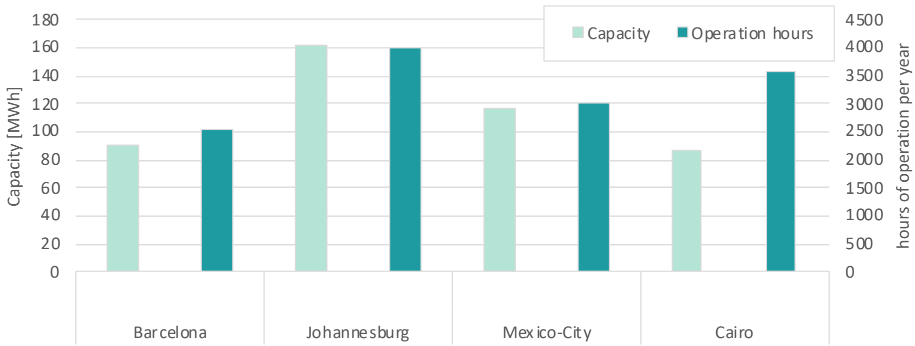

Figure 7: Comparison of annual capacity and operation hours for the four locations.

4.3 Efficiency analysis

Figure 8 shows a comparison of the monthly COP based on the heat supplied to the AdC and the resulting cooling capacity. What is striking is that Cairo has the lowest and therefore worst COP over the course of the year. Due to the high ambient air temperature, the heat rejection temperature affects the COP of the chiller. Mexico-City and Johannesburg show a very similar trend between 0.45 and 0.5. For the Barcelona location, the COP in the first six months is between 0.4 and 0.5. Only in December the COP falls extremely to 0.25. However, it should be mentioned that the cooling yield in this month is only 0.1 MWh.

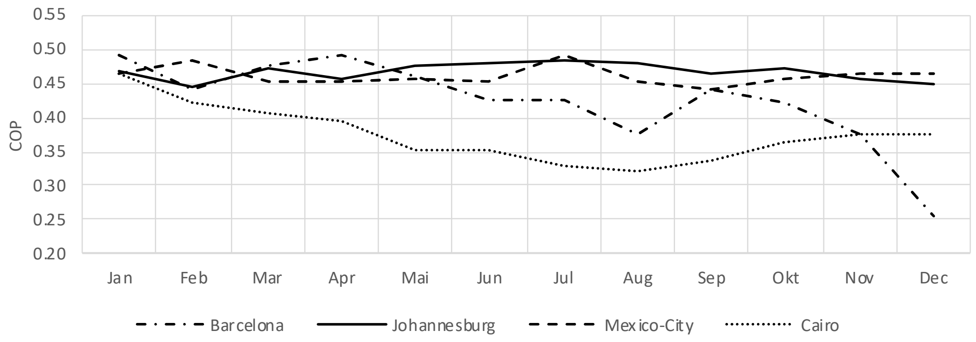

Figure 8: Comparison of annual COP trend per month of AdC**.**

The previously analyzed COP refers to the performance of the AdC, while the EER_{el} refers to the performance of the CC, respectfully to the combination of CC and AdC. The EER_{el} is a technical KPI. It evaluates the chillers' performance and compares the thermal energy output with the electrical energy supplied. As described above, the given EER_{el} of the CC is set to 3.21.

Figure 9 shows the EER_{el} for the Johannesburg location depending on the ambient air temperature. The maximum temperature for the location is slightly above 30 °C. The diagram compares the EER_{el}, which only takes into account thermal output energy of the CC, with the second EERel, which also takes into account the thermal output energy of the AdC. Thanks to the AdC, the CC allows a higher heat rejection temperature and therefore uses less electricity. Thus, the solar cooling system leads to an improvement of the EER_{el} in the system. The diagram shows two main things. On the one hand, the EER_{el} increases as the ambient air temperature decreases. In the case under consideration, the maximum EER_{el} of the CC reaches a value of 7.2. On the other hand, the diagram shows that the EER_{el} increase to higher values by including the AdC. The cooler the ambient air temperature, the greater the change in EER_{el}.

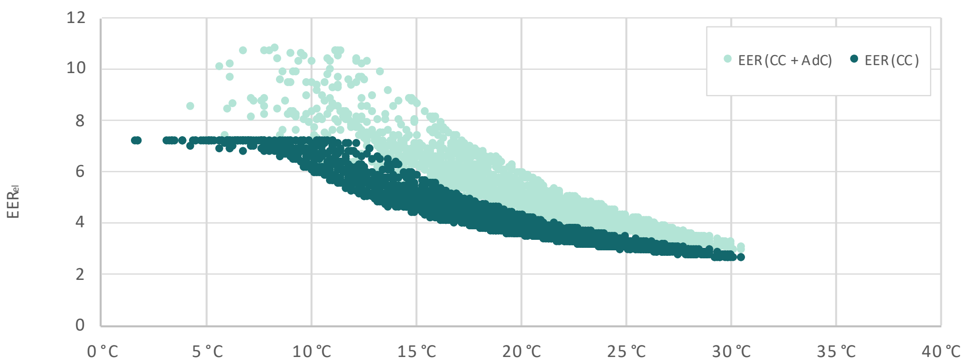

Figure 9: Display of EER_{el} in respect of ambient air temperature for Johannesburg.

Table 4 compares the results of the EER_{el} analysis for each location. The solar cooling system brings best results for the Johannesburg location. The table below also shows that for Egypt, not only the COP of the AdC has the worst performance, but also the EER_{el} of the CC.

Table 4: Comparison of EER_{el} per location for ambient air temperature of 25 °C and above

Location	EER_{el} (CC)	EER_{el} (CC&AdC)	Upgrade
Barelona	2.85	3.25	+14 %
Johannesburg	2.95	3.54	+ 20 %
Mexico-City	2.95	3.54	+ 20 %
Cairo	2.54	2.81	+ 11 %

4.4 Ecological analysis

The other KPI to be analyzed is the potential savings in CO_2 emissions. The potential saving in CO_2 emissions is based on the saved electrical energy consumption of the CCs through the integration of solar cooling. The electricity consumption again is affected by the EER_{el} of the CCs. The EER_{el} varies from one location to another and depends, among other things, but above all, on the ambient air temperature. In addition, the specific CO_2 emissions per kWh electricity vary between the four locations examined. The specific emissions are shown in Table 5. The table contains the OCED average CO_2 factor for comparison purposes. Spain has the lowest CO_2 emissions per kWh_{el} at 247 g/kWh. In contrast, South Africa has the highest CO_2 emissions factor of 926 g/kWh due to the high share of coal (88%) in electricity generation (IEA, 2019). The emission factors of Mexico and Egypt lie between those of Spain and South Africa.

Table 5: Comparison of CO_2 emissions per electric kWh by country.

Country	Spec. electricity-based CO_2-emissions
OECD (OECD, 2022)	432 g/kWh
Spain (2013) (OECD, 2022)	247 g/kWh
South Africa (2013) (OECD, 2022)	926 g/kWh
Mexico (2013) (OECD, 2022)	506 g/kWh
Egypt (2016) (Abdallah et. al, 2017)	630 g/kWh

The saved CO_2 emissions are calculated by dividing the annual cooling capacity by the specific EER_{el} and then multiplying by the individual CO_2 factor. The result of this calculation is shown in Figure 10. The use of solar thermal cooling systems in Johannesburg offers by far the greatest potential for saving CO_2 emissions. The reason for this result lies in two aspects: the Johannesburg location has the best production of cooling capacity and has the highest CO_2 emission per kWh_{el}.

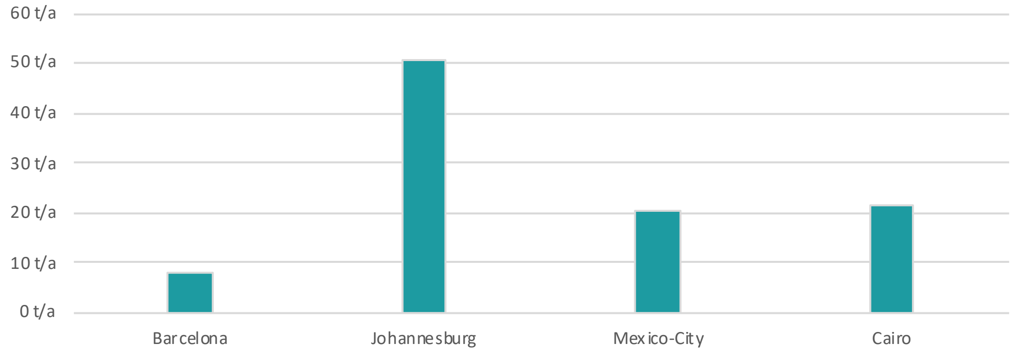

Figure 10: Comparison of potential CO_2 savings.

5. Conclusion

In this work, a solar cooling system for industrial purposes was described and analyzed. Such an innovative system goes beyond the state of the art in industrial heating and cooling supply. Solar systems require a uniform design that meets the requirements of the area of application and of course the climatic and solar conditions of the location. Compared to traditional industrial heating/cooling systems, solar systems tend to be more investment intensive, but are characterized by low operating costs because they are independent of fossil fuels and use solar energy as the primary energy source. For safety reasons in construction site operations, backup systems are still recommended. The technical installation also primarily requires know-how and experts as well as shipping the products. This can be a limitation when it comes to processes in remote areas or developing countries.

The system was simulated in the simulation program TRNSYS 17 to analyze the systems' performance for four locations: Barcelona in Spain, Johannesburg in South Africa, Mexico-City in Mexico and Cairo in Egypt. The weather data analysis showed that Johannesburg has the highest solar radiation, followed by Mexico-City and Cairo. Barcelona has the lowest solar radiation. After analyzing weather data, Johannesburg appears to be the most promising location for industrial solar cooling systems.

The simulation results proved that the most productive, efficient and highest yield results were achieved for the Johannesburg location. The Cairo location has the worst performance due to the highest ambient air temperatures of all four locations. This means that only the combination of ambient air temperature and solar radiation allows conclusions to be drawn about the solar cooling system. A closer look at the AdC's COP_{th} showed that Egypt in particular, but also Spain, have the lowest COP, while the COP for Mexico and South Africa are rather constant throughout the year between 0.45 and 0.50. By integrating solar thermal collectors and thermally driven sorption chillers to the system, the EER_{el} of conventional compression chillers improves by up to 20 %. The environmental analysis came to the conclusion that, with 50 t CO_2 per year, the greatest potential for saving CO_2 emissions lies in South Africa. Mexico and Egypt show a similar result, while Spain already uses renewable energy sources for electricity generation where the potential is therefore the lowest.

Finally, the simulation results and the results of the two analyzed KPI come to the same conclusion: the investigated solar cooling system for industrial purpose examined performs best in Johannesburg, South Africa. In addition, high ambient air temperatures in Cairo reduce the efficiency so much, that even with a higher solar thermal yield, the chiller cooling capacity is lower than in Barcelona.

6. References

Abdallah, L. and El-Shennawy, T., 2017. Evaluation of CO_2 emissions form electricity generation in Egypt: Present Status and Projections to 2030.

Eurostat, 2018. Energy balance sheets 2016 DATA: 2018 edition.

Frazzica, A. et. al, 2020. Renewable Heating and Cooling Solutions for Buildings and Industry. Proceedings, 65, 16; DOI: 10.3390/proceedings2020065016.

IEA, 2019. Data and statistics. Available online: https://www.iea.org/data-and-statistics/data-tables?country=SOUTHAFRIC&energy=Electricity&year=2019 (accessed on 26 November 2022).

Jakob, U. and Kiedaisch, F., 2019. Analysis of a solar hybrid cooling system for industrial applications. Proceedings of ISES Solar World Congress 2019; DOI:10.18086/swc.2019.55.07.

Monforti-Ferrario, F., Dallemand, J.-F., Pinedo Pascua, I., Motola, V., Banja, M., Scarlat, N., Medarac, H., Castellazzi, L., Labanca, N., Bertoldi, P., Pennington, D., Goralczyk, M., Schau, E. M., Saouter, E., Sala, S., Notarnicola, B., Tassielli, G., Renzulli, P., 2015. Energy use in the EU food sector: State of play and opportunities for improvement. European Commission: Institute for Energy and Transport and Institute for Environment and Sustainability.

OECD, 2022. Compare your country. Available online: https://www2.compareyourcountry.org/climate-policies?cr=oecd&lg=en&page=2&visited=1# (accessed on 26 November 2022).

Pachauri, R.K. and Meyer, L.A. (eds.), 2014. Climate Change 2014: Synthesis Report. Contribution of Working Groups I, II and III to the Fifth Assessment Report of the Intergovernmental Panel on Climate Change IPCC, Geneva, Switzerland, 151 pp.

UNIDO, 2010. Renewable Energy in Industrial Applications – An assessment of the 2050 potential.